Atlas of Formability

XD Composite

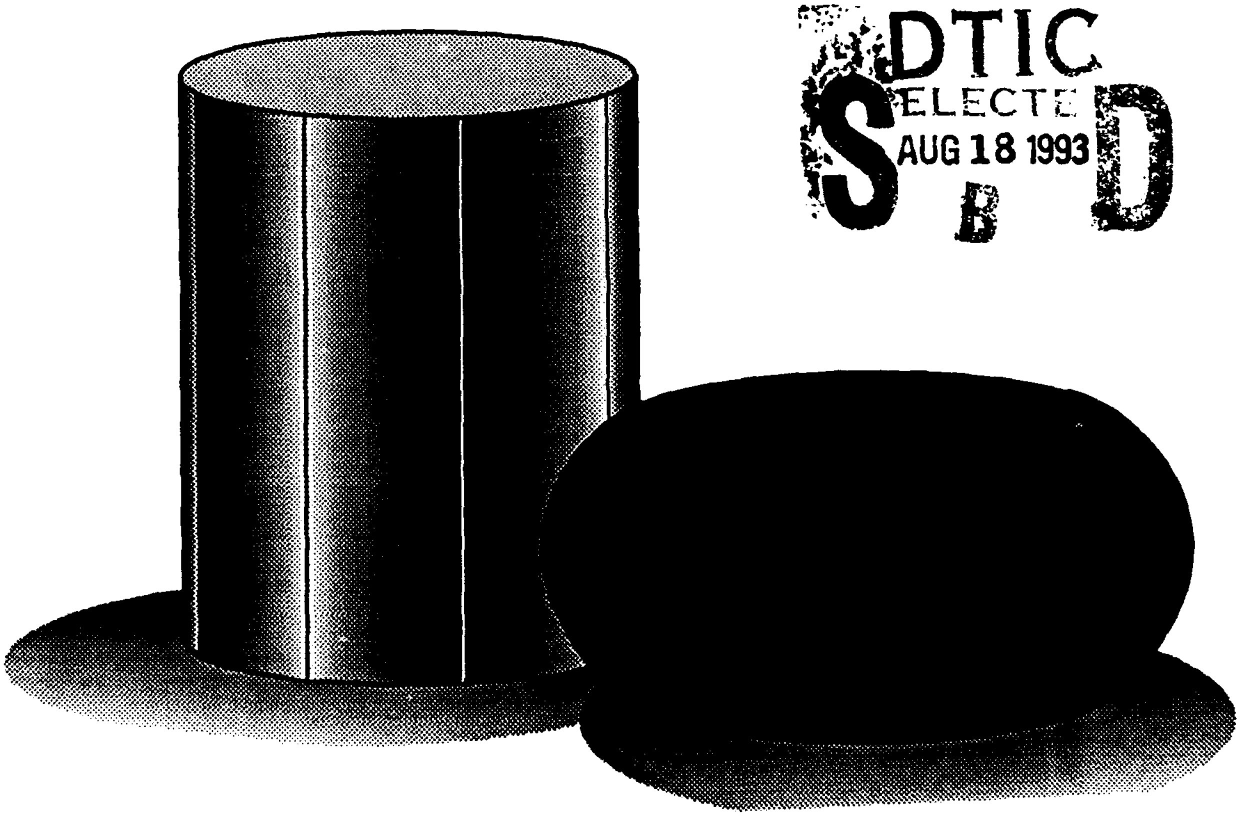

NCEMT

ATLAS OF FORMABILITY

Al-TiC XD COMPOSITE

by

Howard A. Kuhn

National Center for Excellence in Metalworking Technology
1450 Scalp Avenue
Johnstown, PA 15904

for

Naval Industrial Resource Support Activity
Building 75-2, Naval Base
Philadelphia, PA 19112-5078

July 31, 1991

REPORT DOCUMENTATION PAGE

Form Approved
OMB No. 0704-0188

1. AGENCY USE ONLY *(Leave blank)*

2. REPORT DATE
July 31, 1991

3. REPORT TYPE AND DATES COVERED
Final, April 30, 1991 - July 31, 1991

4. TITLE AND SUBTITLE
Atlas of Formability
Al-TiC XD Composite

5. FUNDING NUMBERS
C-N00140-88-C-RC21

6. AUTHOR(S)
Howard A. Kuhn

7. PERFORMING ORGANIZATION NAME(S) AND ADDRESS(ES)
National Center for Excellence in Metalworking Technology (NCEMT)
1450 Scalp Avenue
Johnstown, PA 15904

8. PERFORMING ORGANIZATION REPORT NUMBER

9. SPONSORING/MONITORING AGENCY NAME(S) AND ADDRESS(ES)
Naval Industrial Resources Support Activity
Building 75-2, Naval Base
Philadelphia, PA 19112-5078

10. SPONSORING/MONITORING AGENCY REPORT NUMBER

11. SUPPLEMENTARY NOTES

12a. DISTRIBUTION/AVAILABILITY STATEMENT

12b. DISTRIBUTION CODE

13. ABSTRACT *(Maximum 200 words)*

In this investigation, flow behavior of Al-TiC XD Composite was studied by conducting compression tests over a range of temperatures and strain rates. The workability of the material was determined for each test condition. Some corresponding microstructure was also examined. These data are essential in metalworking process design or finite element analysis of high temperature deformation.

14. SUBJECT TERMS
Al-TiC XD Composite, High Temperature Deformation, Metalworking

15. NUMBER OF PAGES
27

16. PRICE CODE

17. SECURITY CLASSIFICATION OF REPORT	18. SECURITY CLASSIFICATION OF THIS PAGE	19. SECURITY CLASSIFICATION OF ABSTRACT	20. LIMITATION OF ABSTRACT
Unclassified	Unclassified	Unclassified	

TABLE OF CONTENTS

Introduction:

Process development for XD composites has been underway for several years. Emphasis has been placed on the aluminum matrix containing titanium carbide particles having an average particle size of 2.8 micrometers. To enhance the understanding of material characteristics for deformation processing, a limited test program on workability was carried out.

Two alloy grades of XD composite bar stock containing 15% and 25% titanium carbide (TiC) were received for workability testing. Test parameters were chosen to simulate the extrusion data supplied by Martin Marietta Laboratories. The following program plan defines and demonstrates the compressive workability study for the evaluation of the XD composite material.

Program Plan:

A program plan was carried out to develop the necessary information for fracture prediction during processing of XD composite materials, including:

1. Sample preparation
2. Grid line measurement
3. Workability studies
4. Metallographic investigations of test specimens

In Phases 1 & 2, samples were prepared from the corresponding bar stock into usable samples for data collection.

In Phase 3, compression deformation tests were conducted on an instrumented MTS machine configured for isothermal workability and flow stress testing. Axial compression tests with frictional constraint were used to generate the material workability strain limits.

In Phase 4, metallographic investigations were conducted using a Leco image enhanced metallograph and a Tracor Northern Scanning Electron Microscope.

Background:

A convenient way to describe and measure the likelihood of ductile fracture for a given material is a property called workability. Since internal ductile fractures cannot be detected except by sectioning the bars, fracture maps of a given process are expensive to prepare. Furthermore, each process requires its own set of fracture maps. An alternative is to use results of simple tests that apply universally to a variety of processes.

One such test is the upset test on cylindrical specimens with frictional constraint. The typical strain path for a point on the free surface of such an upset specimen is demonstrated in Figure 1. Barreling occurs with rough dies and small aspect ratios; therefore, the tensile strain component (e1) increases more rapidly than the axial compressive strain (e2). If enough strain is applied, these samples will develop cracks at the equator of their free surfaces. A scatter plot can be made which shows the axial compressive strain (e2) versus the circumferential strain (e1) for both fractured and unfractured samples. This plot is useful for determining the limits of plastic working in the presence of a biaxial stress state. Additional points can be obtained by varying sample heights and friction conditions of the die surfaces. A curve representing the onset of ductile fracture is typically a straight line having a slope of -0.5, which matches the slope of the curve for homogeneous compression.[1]

An example of such a curve is shown in Figure 2. The straight line represents the upper limit of workability for the material under the tested conditions. This line is called the fracture strain line and is applicable to any process exhibiting a biaxial stress state. At strain conditions below this line, fracture is unlikely, while strain conditions above this line will result in a high probability of ductile fracture. Such curves, then, form the basis for comparing material process parameters to find the most favorable conditions for a given process. These process parameters may include temperature, strain rate, and grain size. Compressive workability testing is very useful for describing the ability of a material to withstand biaxial stress states.

---

[1] Kuhn, Howard A., "Workability Theory and Application in Bulk Forming Processes," Metals Handbook, ninth edition, Volume 14: Forming and Forging, ASM International, pp 388-404.

Experimental Approach:

Workability tests were conducted on specimens from two alloys of XD composite material. Materials tested included 15% and 25% (by volume) TiC in an aluminum matrix. In all cases, the test specimens were cylindrical with their axes aligned with the axes of the original bars to assure similar orientation between stress direction and microstructure features in both the bar stock and the test specimens.

The 15% and 25% TiC aluminum matrix composite materials were machined into samples having a diameter of 0.5 inches. The stock bars were also machined so that there was an equal number of specimens corresponding to a height of 0.5 inches and 0.875 inches from both XD composite grades. Thermocouple holes were drilled radially at mid-height. Grid lines spaced 0.05 inches apart were machined onto the circumferential surface of the samples. The grid line spacing was measured before and after testing.

Due to the number of samples available for testing, three temperatures (600, 700, and 800 F) and one strain rate (1.0/sec) were chosen for the material evaluation. Both alloys were tested using specimens of both heights. Smooth and knurled platens were used to vary friction conditions on the contact surfaces. The percentage of deformation was also controlled thereby varying the strain placed on the material during testing.

Several samples were investigated using the metallograph and SEM to characterize the TiC distributions.

Results and Discussion:

1) Upset Tests

Tables 1 through 5 list the test parameters and results for the 15% and 25% TiC alloys, and Figures 3 through 8 present the mechanical test results. Fracture data at the three different test temperatures for the two different composite samples are presented.

These tests were conducted with two different sets of compression dies. One set had a smooth tooling surface while the

other was knurled to increase the tensile circumferential strain by preventing the movement of the surface of the test specimen.

The results included show a fracture band where incipient cracking for failure would occur during processing at these levels of total strain. A specific fracture line could not be provided owing to the limited number of samples which were available. However, sufficient test results were obtained to map out a fracture band which should be used as a guideline in the processing of the composites.

Figures 3 through 8 show the workability data for the two XD composites with 15% and 25% TiC. As the data indicate, there is an improvement in the workability of these materials from 600 to 800 F. The bands drawn on these figures indicate an area where fracture would be a possibility during forming of the composites. To insure that no fractures occur during processing, these materials should be processed below this band.

This workability criterion is for the formation of surface cracks only; as a result, internal cracks may or may not be formed at these levels of deformation, depending on stress state at the interior of the composite.

Since all of the curves for XD composite material have slopes of -0.5, these results can be summarized by y-intercepts (the value of circumferential [hoop] strain at zero axial strain) at the lower band of the incipient cracking zone. Summary comparisons are presented in Table 5. The data indicate higher temperature increases the workability for the 15% and 25% TiC materials. The table also shows that the variation between the two materials for the development of ductile fractures is quite small.

2) Metallography

Four of the XD composite samples with 15% volume fraction TiC particles were sectioned, mounted and etched in Keller's reagent for 15 minutes.

Figures 9 through 11 show several photomicrographs of tested samples. The most notable pattern in the composite is the inhomogeneous distribution of TiC particles. With the difference of material characteristics between the aluminum alloy matrix and the

TiC particles, this variation is not surprising. Analysis of the tested specimens had shown areas of surface failure through the "blow-out" of material. These areas occur at locations different from tearing caused by fracture during testing. A typical "blow-out" region is shown in Figure 12.

Metallographic investigation of these blow outs shows that the areas along the outer diameter of the samples is lower in concentration of TiC particles than the bulk of the sample. Some development of an image analysis routine to determine the particle concentration was performed and these results confirm the visual observation.

It is *presumed* that the lower number of particles at the outer diameter is a result of some shear and flow effect as a result of extrusion. One way to confirm this would be to evaluate the variation in particle distribution in a bar of unmachined XD composite material. The lower number of particles yields a localized area of lower mechanical strength which could lead to surface failure as a result of tensile stresses.

The metallographic analysis also shows some acicular particles, some areas free of particles, and, apparently two different matrix phases.

3) SEM Analysis

SEM photomicrographs of various fracture surfaces are enclosed. Figures 13 and 14 clearly show surface cracks which appear to be the result of tearing the matrix material. Figures 15 and 16 show SEM photomicrographs of the "blow-out" areas. It appears that fracture in the "blow-out" areas is the result of brittle fracture, as opposed to the ductile cracking described above for matrix material. The data produced to date show no conclusive results. A more comprehensive study of the chemistry variation and fracture areas is needed to determine micromechanical and microchemical mechanisms in the fracture processes.

Future work:

Future work should focus on the possibility of microphase separation and precipitation of copper-rich and copper-depleted structures. This issue could be resolved by performing microchemical mapping over a wide area of the composite material and across what appears to be two different phases.

In addition, flow stress curves and actual verification of the fracture lines by testing at various rates of strain would yield more information on the workability of these materials.

Also of interest is the possibility of particulate depletion near the exterior surface of the extruded bar. A thorough investigation of the particle distribution in cast ingots as well as in extruded bars would allow the determination of the natural variation in particle distribution and whether any variation was a result of forming operations.

To determine the particle distribution and the existence of multiple phases, additional etchants need to be evaluated.

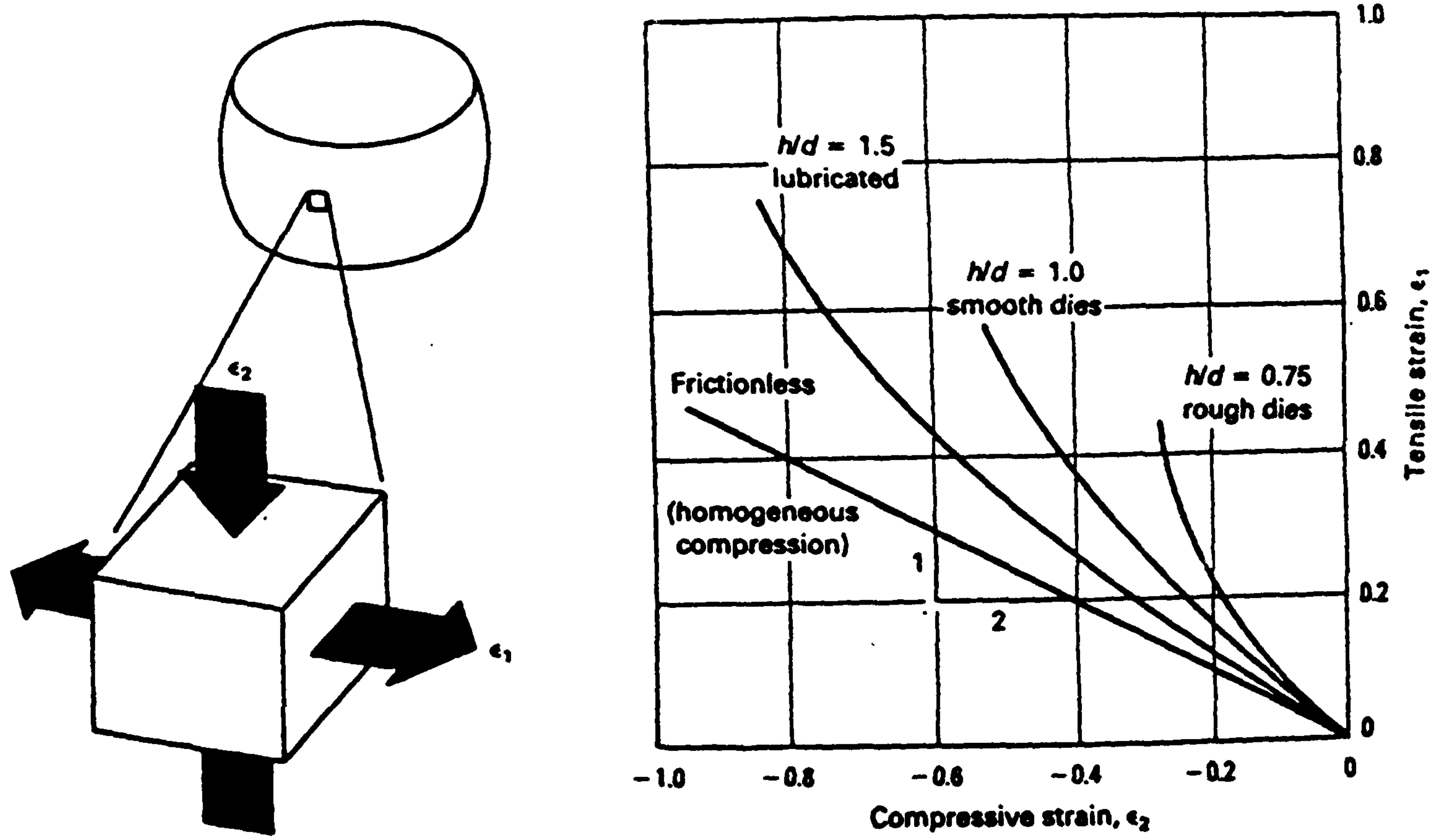

(a) (b)

Figure 1: Localized Strains on the Bulging Cylindrical Surface of an Upset Test (a) and Their Variation With Aspect Ratio and Friction Conditions (b) [*Source*: Kuhn, Howard A., "Workability Theory and Application in Bulk Forming Processes," Metals Handbook, niinth edition, Volume 14: Forming and Forging, ASM International, pp 388-404.]

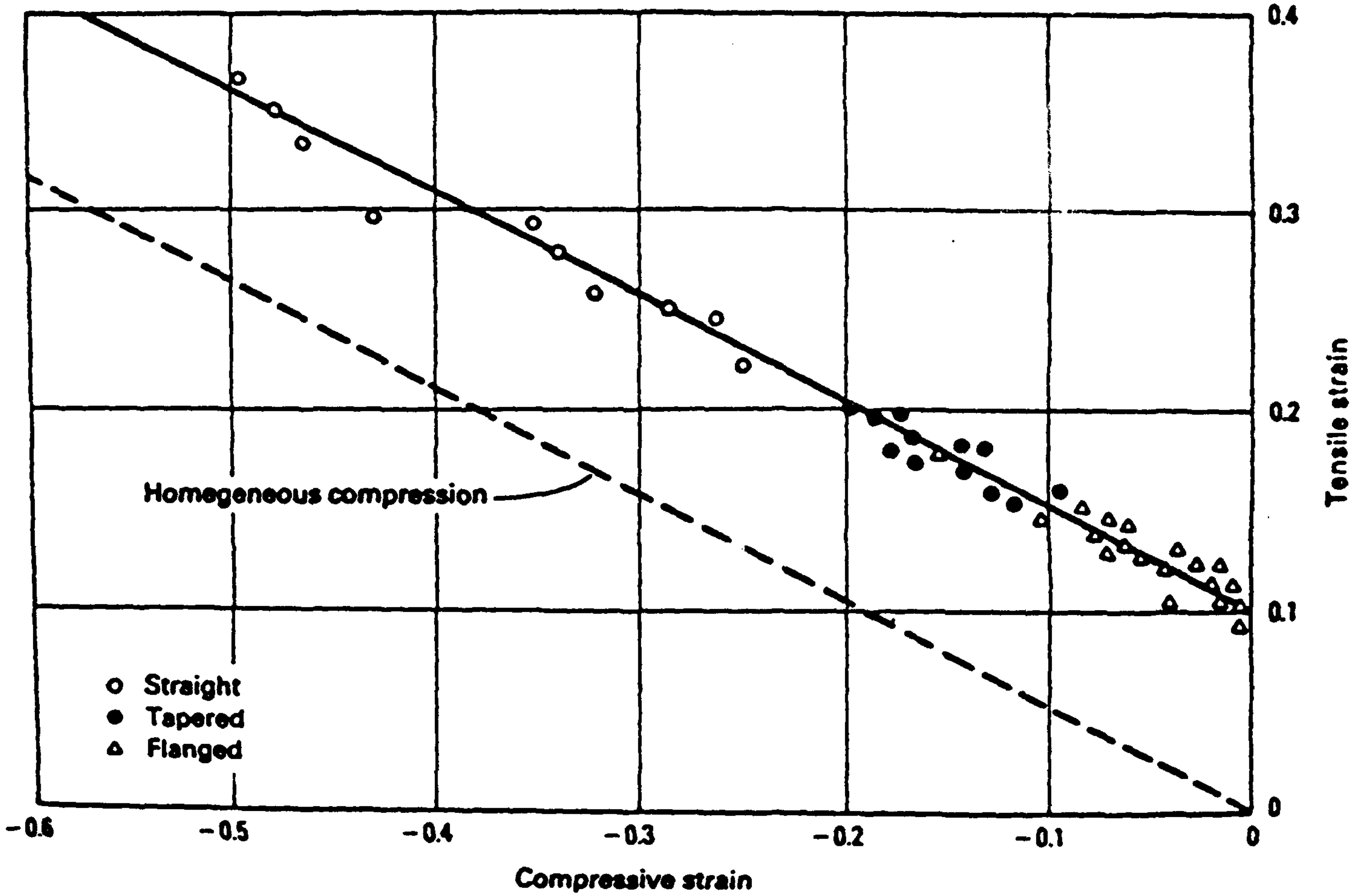

Figure 2: Fracture Locus for Aluminum Alloy 2024-T351 at Room Temperature. [Source: Kuhn, Howard A., "Workability Theory and Application in Bulk Forming Processes," Metals Handbook, niinth edition, Volume 14: Forming and Forging, ASM International, pp 388-404.]

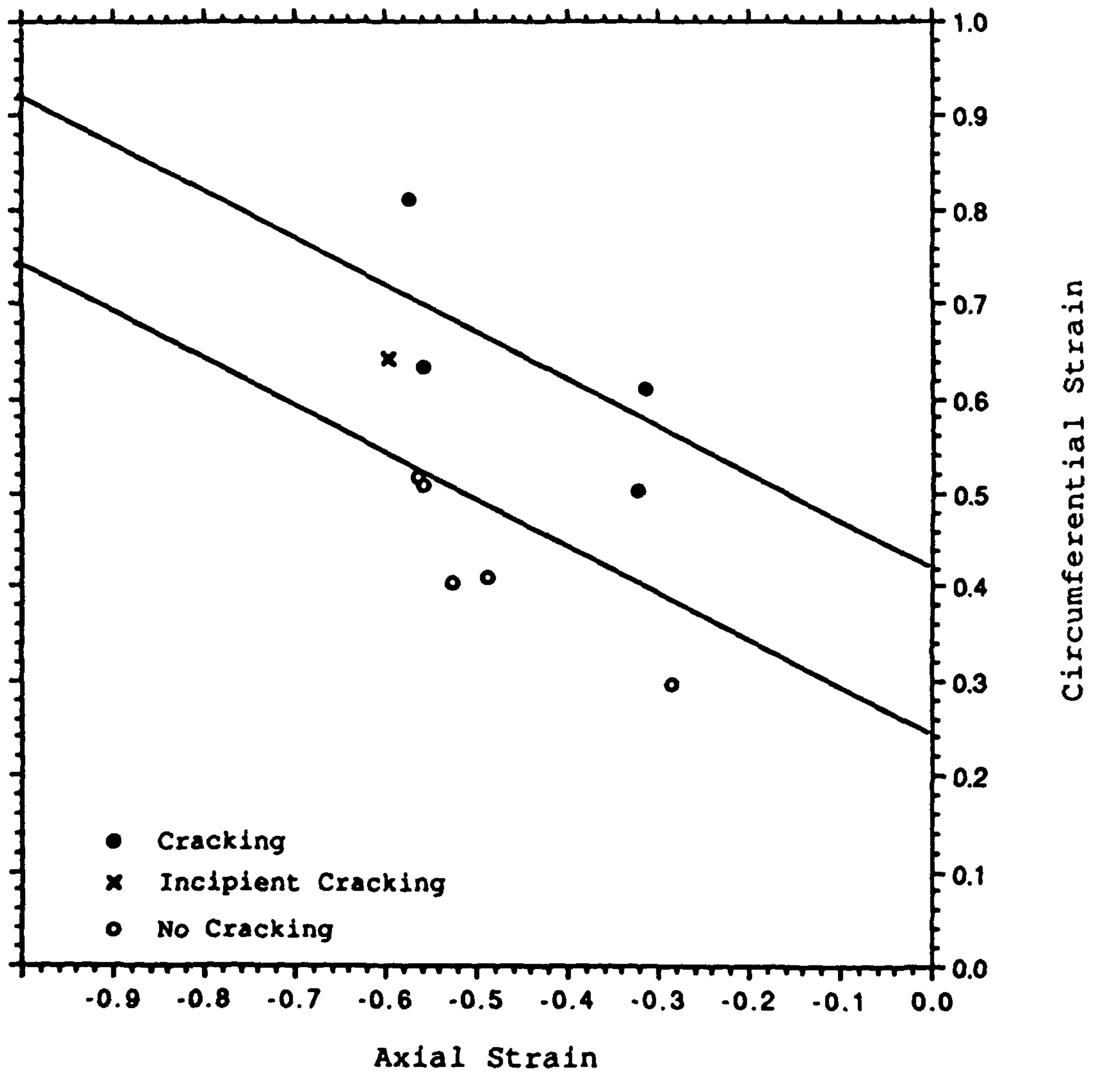

Figure 3: Workability for XD Composite w/15% TiC at 600 F

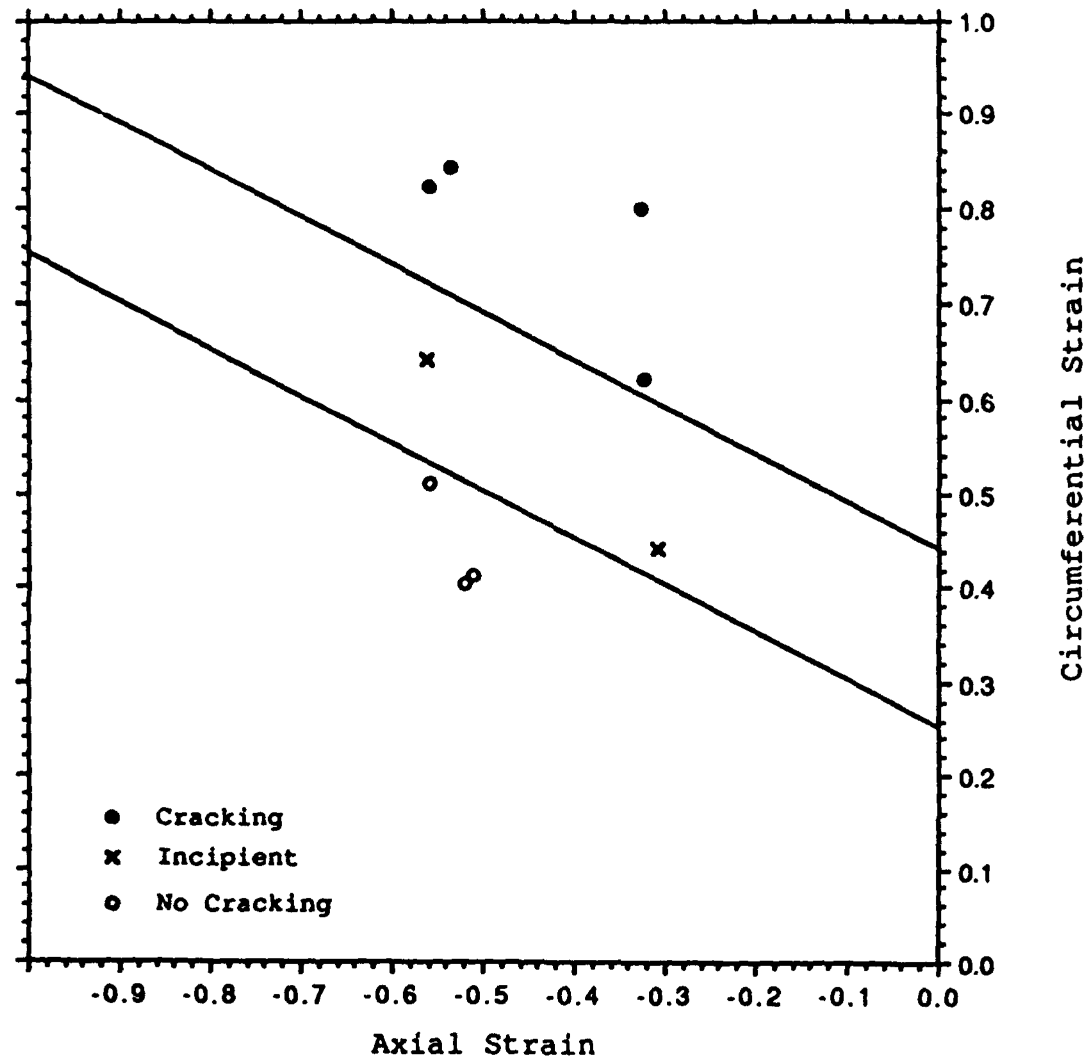

Figure 4: Workability for XD Composite w/15% TiC at 700 F

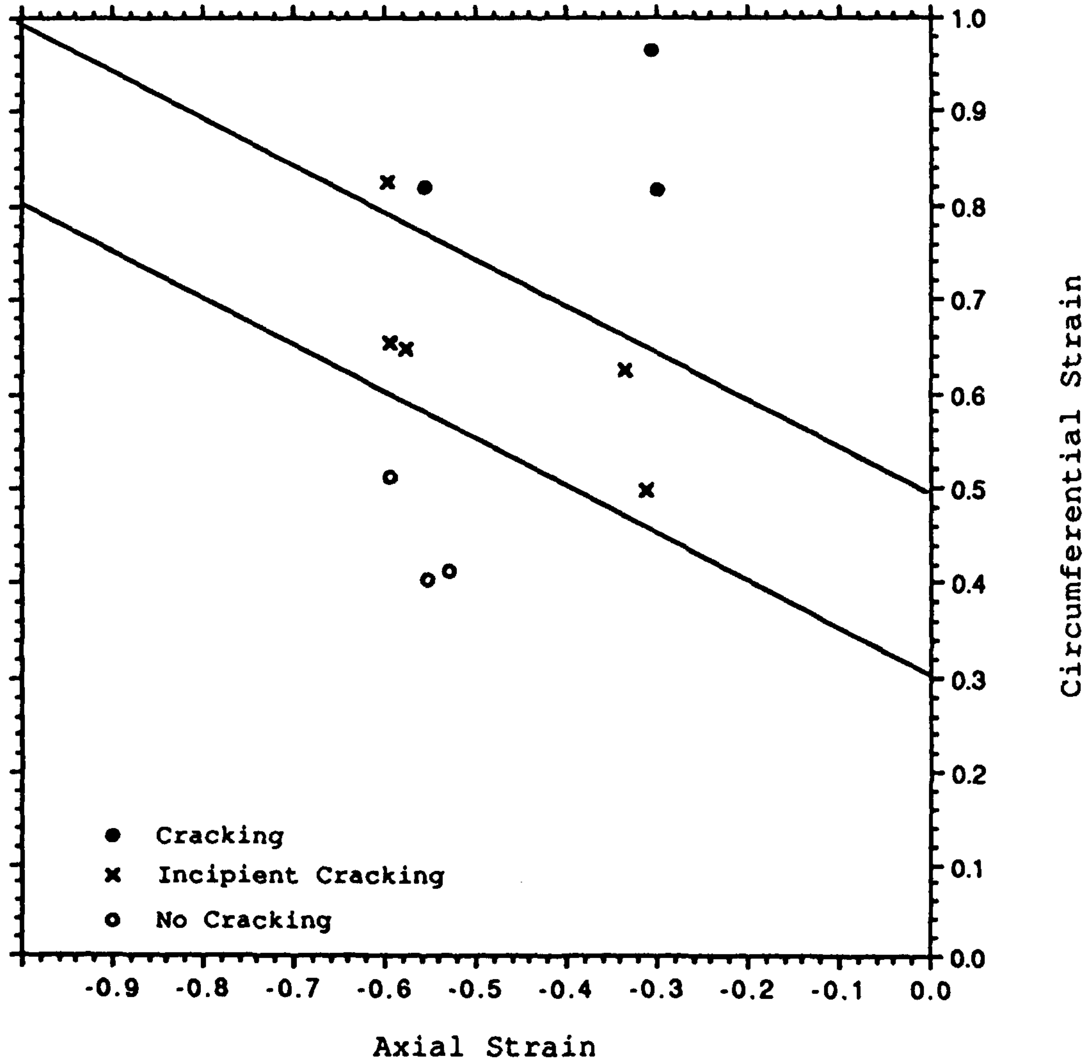

Figure 5: Workability for XD Composite w/15% TiC at 800 F

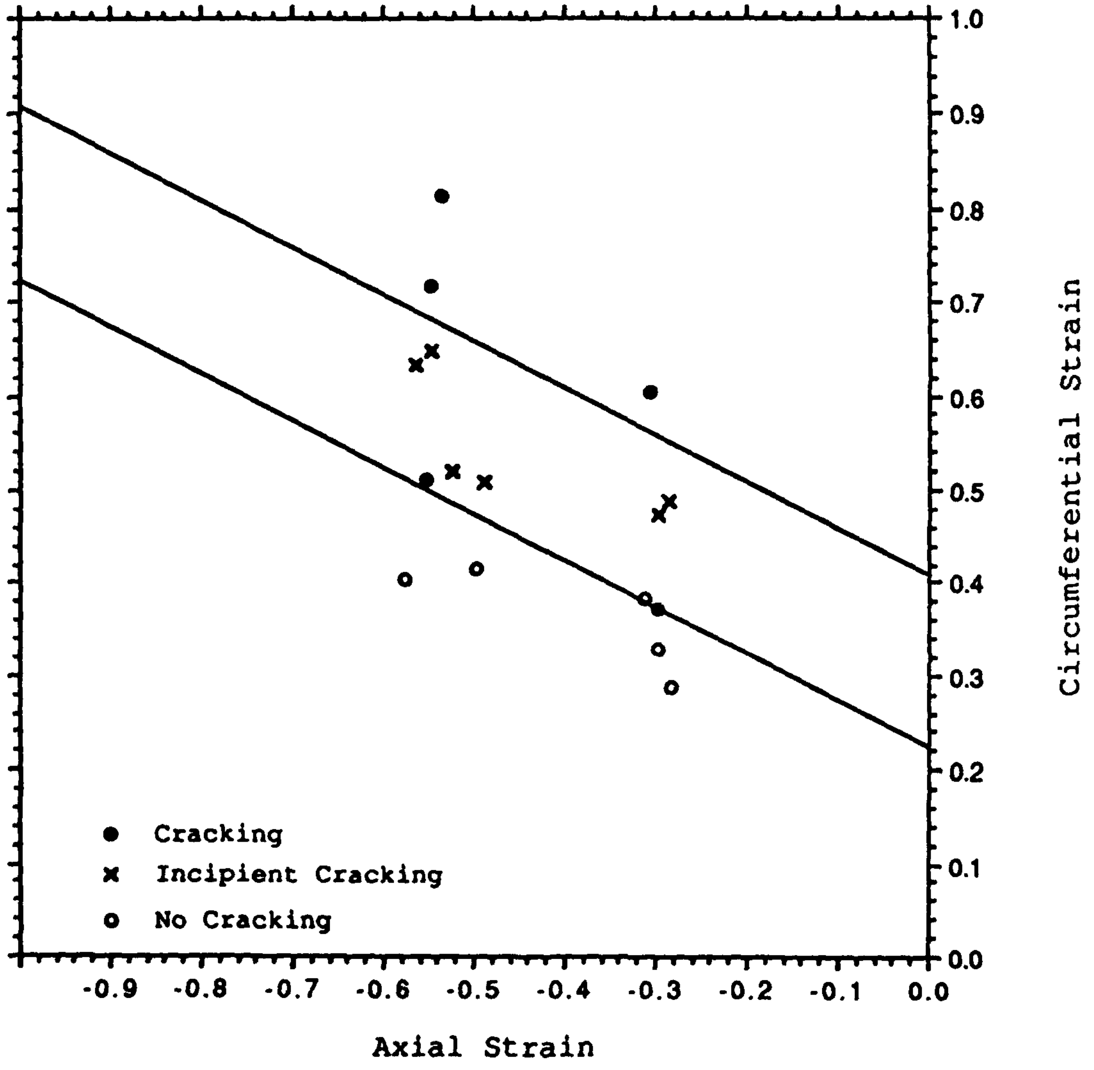

Figure 6: Workability for XD Composite w/25% TiC at 600 F

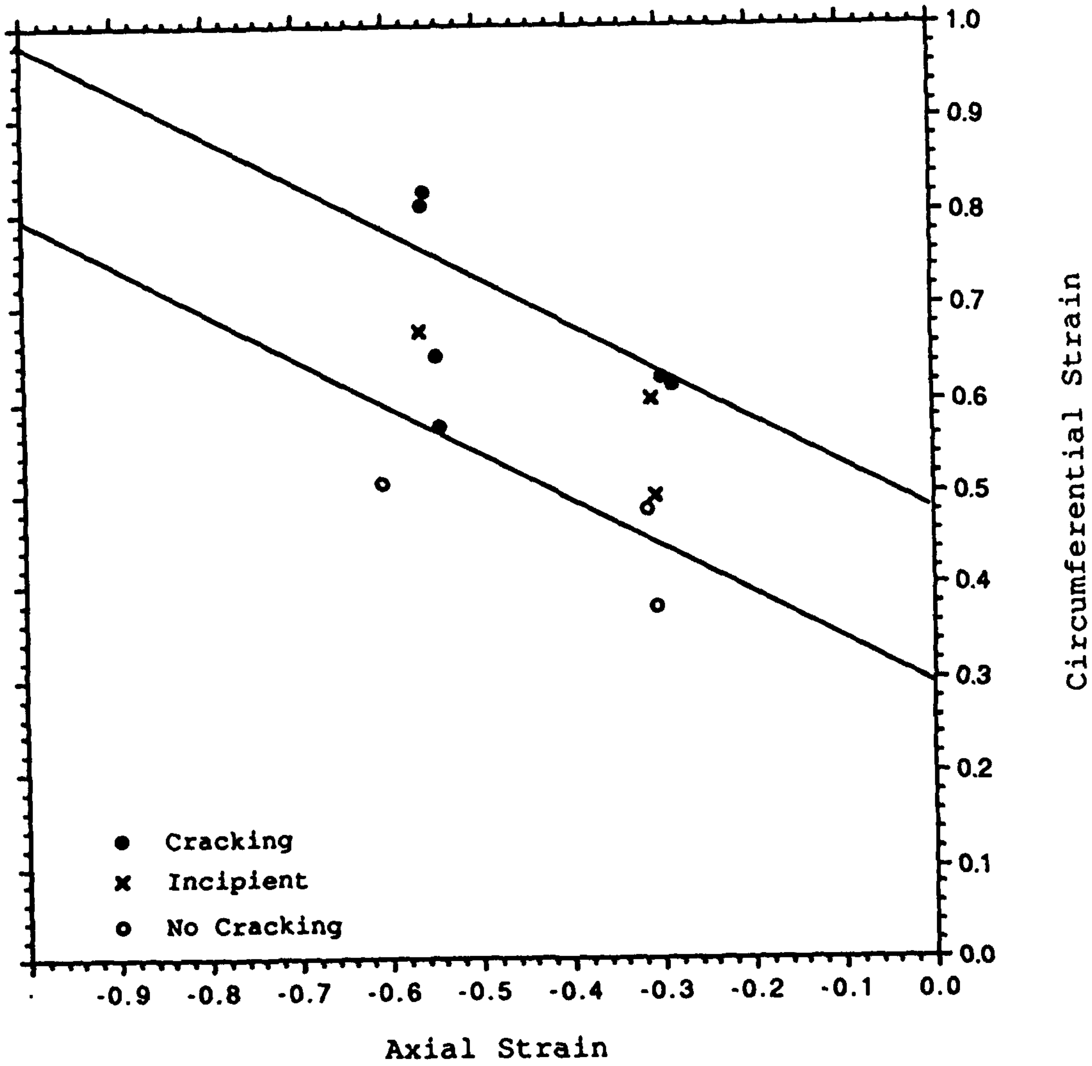

Figure 7: Workability for XD Composite w/25% TiC at 700 F

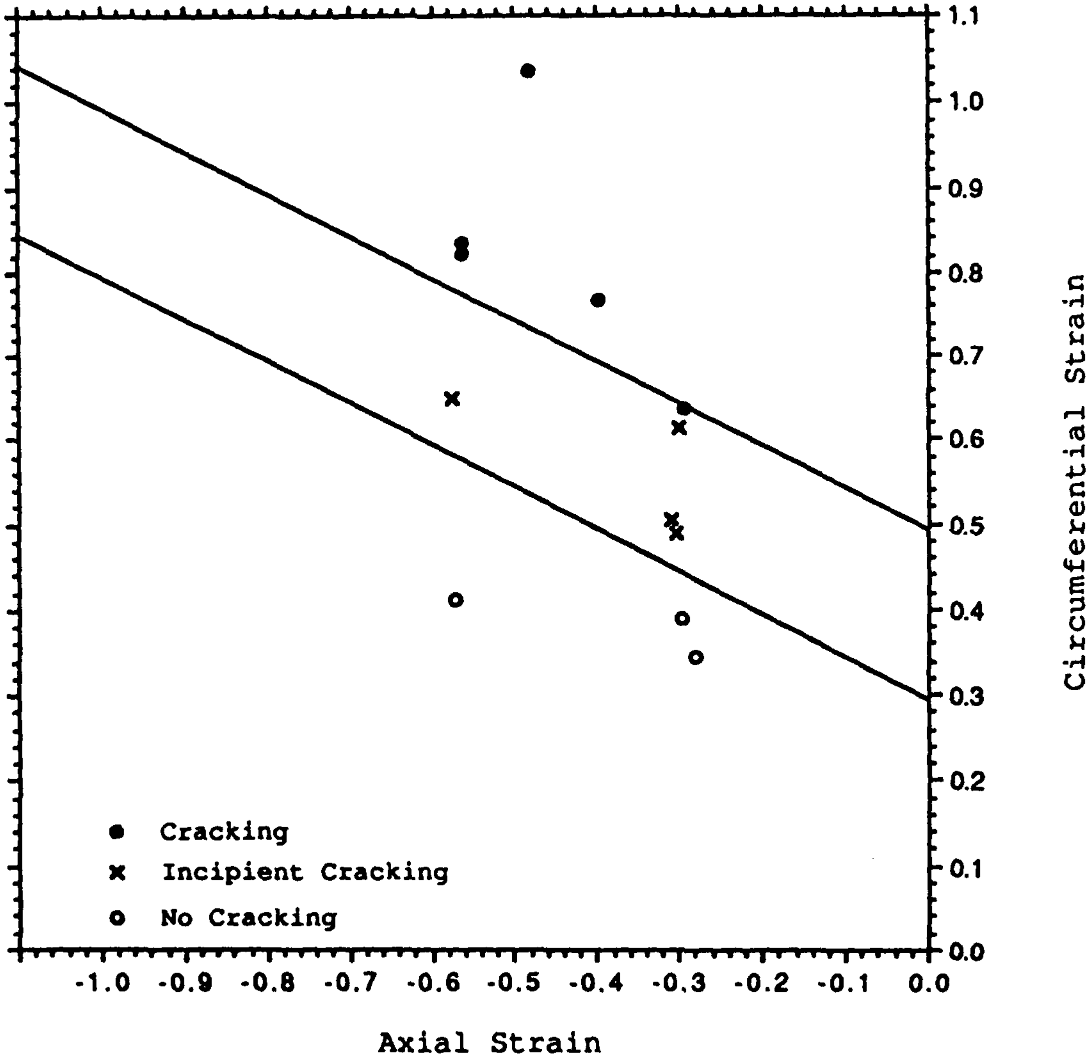

Figure 8: Workability for XD Composite w/25% TiC at 800 F

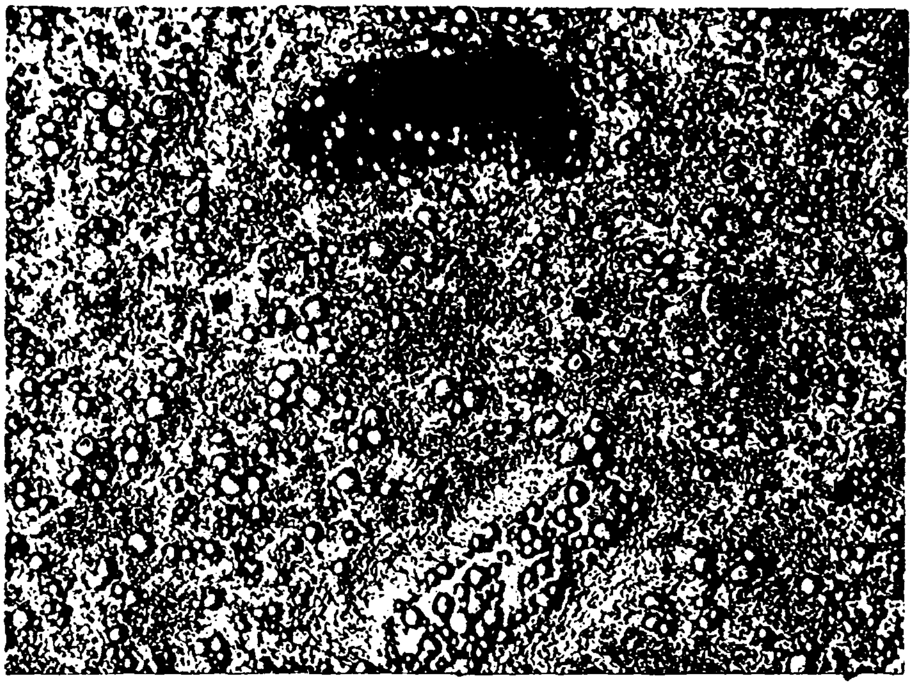

Figure 9: XD composite with 15% TiC (sample #36). Region at the top shows void/poor homogeneity. Region at the bottom shows particle clumping. Kellers Etchant. 500X.

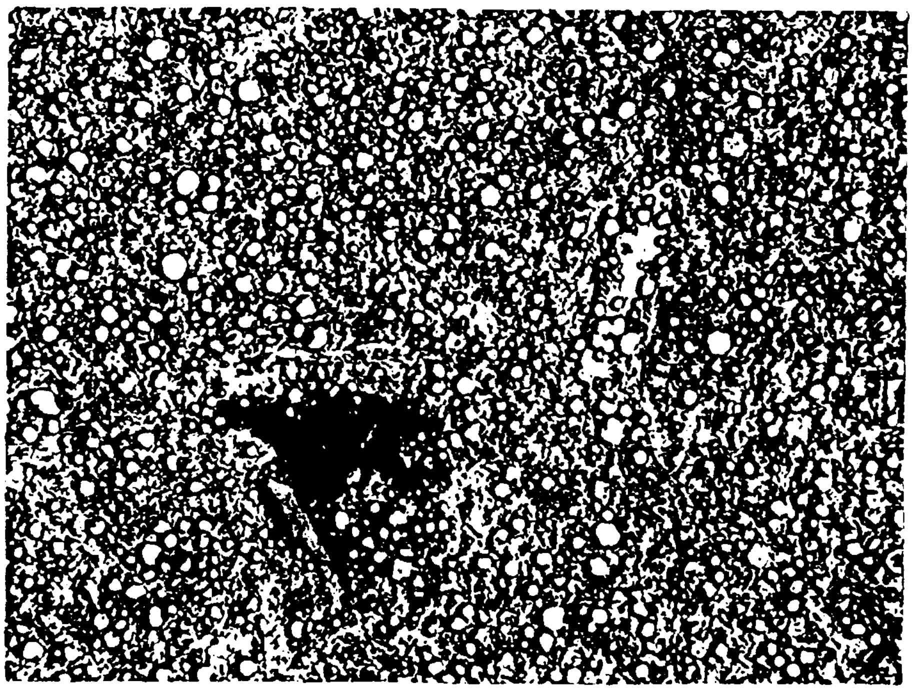

Figure 10: XD composite with 15% TiC (sample #25). Region at the bottom shows void/poor homogeneity and acicular particle. Kellers Etchant. 500X.

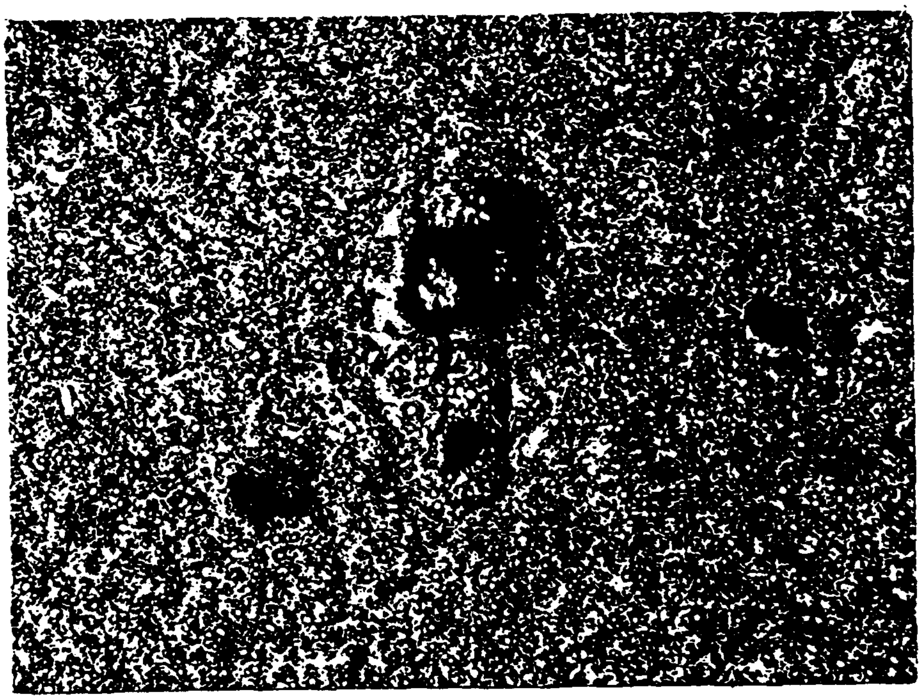

Figure 11: XD composite with 15% TiC (sample #32). Region in the center shows void/poor homogeneity, acicular particles and particle clumping. Kellers Etchant. 200X.

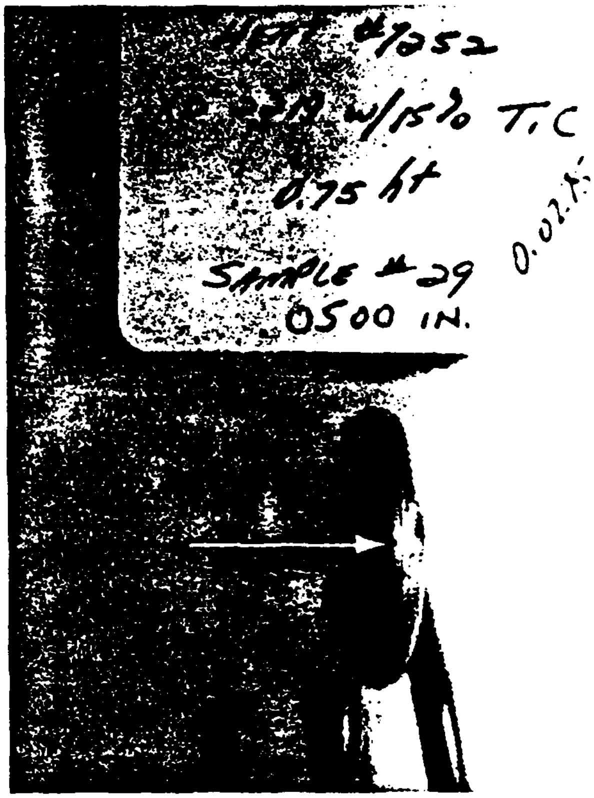

Figure 12: XD composite with 15% TiC (samples #29). Arrow shows the "blow-out" feature present after testing. 4X.

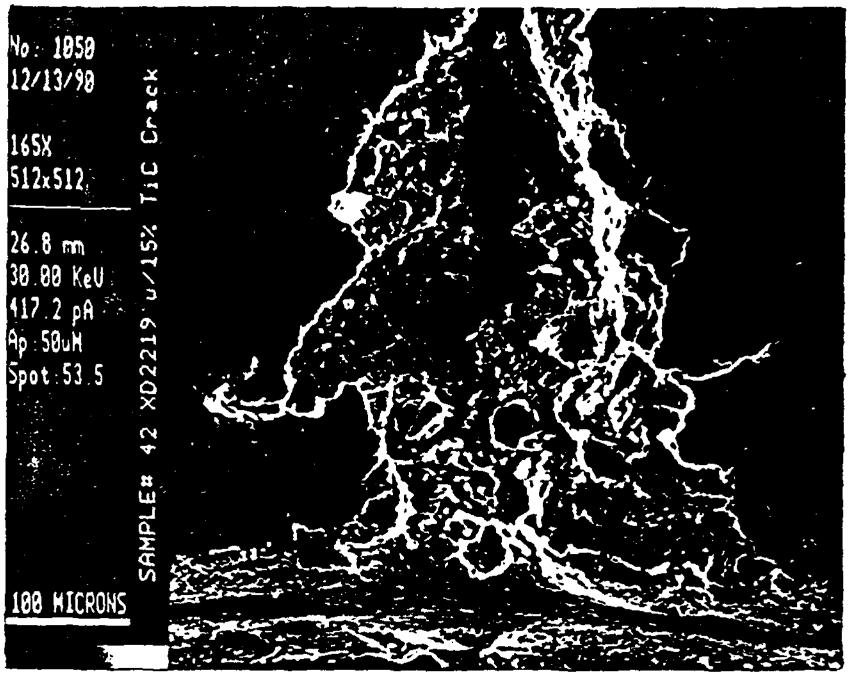

Figure 13: XD composite with 15% TiC (sample #42). SEM photomicrograph showing a cracked surface at 165X.

Figure 14: XD composite with 15% TiC (sample #42). SEM photomicrograph at 1000X. Clearly shows that the cracked surface was the result of tearing the matrix material.

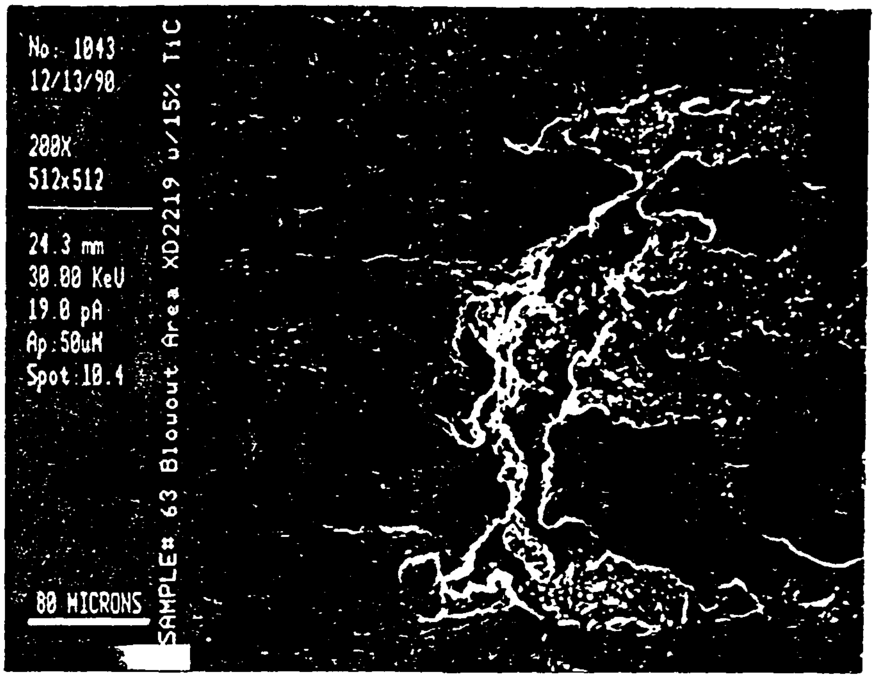

Figure 15: XD composite with 15% TiC (sample #63) SEM photomicrograph showing a "blow-out" at 200X.

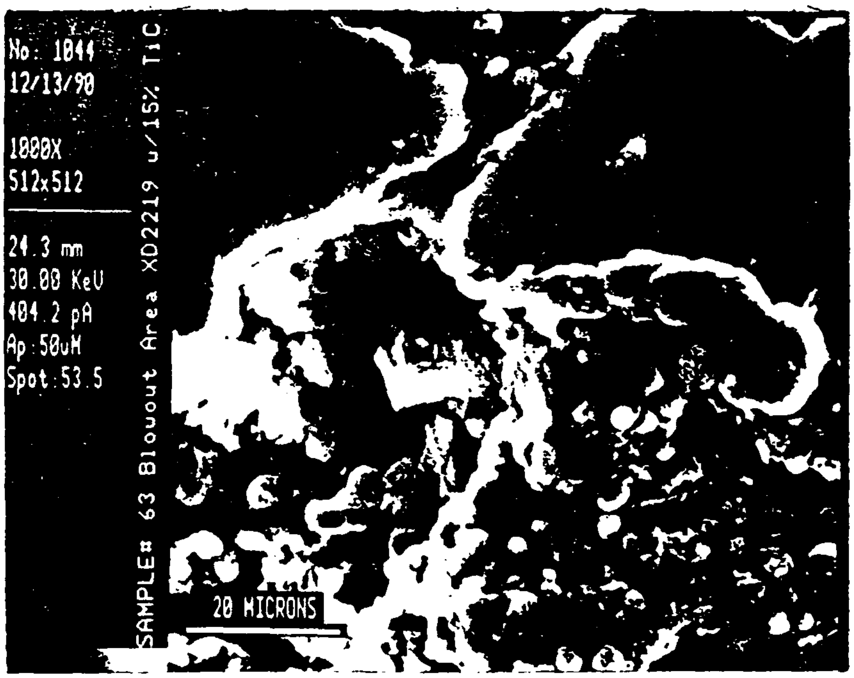

Figure 16: XD composite with 15% TiC (sample #63) SEM photomicrograph showing a "blow-out" at 1000X. Shows mechanism of fracture different from cracked surface.

Table 1: X-D Composites 15% TiC

Sample No.	Heat #	Sample Size	% Red.	S.R. 1/sec	Temp. deg. F	Diameter		Scribe Lines		Platens	Comments
						Initial	Final	Initial	Final		
1	7252	0.500	50	1.0	500	0.500	0.730			Smooth	No Cracking
2	7252	0.500		1.0	500	0.500	0.956			Smooth	Error in Testing
3	7252	0.500	40	1.0	500	0.500	0.670			Smooth	No Cracking
4	7252	0.500	60	1.0	500	0.500	0.806			Smooth	Incipient Cracking
5	7252	0.500	65	1.0	500	0.500	0.856			Smooth	Cracking
6	7252	0.500	65	1.0	600	0.500	0.864			Smooth	Cracking
7	7252	0.500	70	1.0	600	0.500	0.920			Smooth	Cracking
8	7252	0.500	80	1.0	700	0.500	1.084			Smooth	Cracking
9	7252	0.500	80	1.0	700	0.500	1.112	0.0500	0.0361	Smooth	Cracking
10	7252	0.500		1.0	700	0.500		0.0500		Smooth	Error in Testing
11	7252	0.500	90	1.0	800	0.500	1.313	0.0494	0.0364	Smooth	Cracking
12	7252	0.500	80	1.0	800	0.500	1.132	0.0499	0.0370	Smooth	Cracking
13	7252	0.500	60	1.0	600	0.500	0.828	0.0499	0.0361	Smooth	Cracking
14	7252	0.500	70	1.0	700	0.500	0.931	0.0500	0.0362	Smooth	Cracking
15	7252	0.500	70	1.0	800	0.500		0.0500		Smooth	Error in Testing
16	7252	0.500	70	1.0	800	0.500	0.935	0.0500	0.0358	Smooth	Incipient Cracking
17	7252	0.500	55	1.0	700	0.500	0.778	0.0499	0.0366	Smooth	Incipient Cracking
18	7252	0.500	40	1.0	600	0.500	0.672	0.0500	0.0376	Smooth	No Cracking
19	7252	0.500	70	1.0	600	0.500	0.921	0.0497	0.0363	Smooth	Cracking
20	7252	0.500	60	1.0	800	0.500	0.822	0.0500	0.0366	Smooth	Incipient Cracking

Table 2: X-D Composites 15% TiC

Sample No.	Heat #	Sample Size	% Red.	S. R. 1/sec	Temp. deg. F	Diameter Initial	Diameter Final	Scribe Lines Initial	Scribe Lines Final	Platens	Comments
21	7252	0.875	50	1.0	600	0.500	0.754	0.0501	0.0308	Smooth	No Cracking
22	7252	0.875	60	1.0	600	0.500	0.838	0.0500	0.0284	Smooth	No Cracking
23	7252	0.875	70	1.0	600	0.500	0.951	0.0501	0.0276	Smooth	Incipient Cracking
24	7252	0.875	80	1.0	600	0.500	1.125	0.0499	0.0281	Smooth	Cracking
25	7252	0.875	50	1.0	800	0.500	0.756	0.0500	0.0295	Smooth	No Cracking
26	7252	0.875	80	1.0	700	0.500	1.138	0.0499	0.0285	Smooth	Cracking
27	7252	0.875	50	1.0	700	0.500	0.755	0.0500	0.0300	Smooth	No Cracking
28	7252	0.875	80	1.0	700	0.500	1.163	0.0499	0.0292	Knurled	Cracking
29	7252	0.875	80	1.0	800	0.500	1.143	0.0500	0.0275	Knurled	Incipient Cracking
30	7252	0.875	90	1.0	700	0.500	1.393	0.0501	0.0285	Smooth	Cracking
31	7252	0.875	70	1.0	800	0.500	0.963	0.0500	0.0276	Smooth	Incipient Cracking
32	7252	0.875	70	1.0	600	0.500	0.943	0.0500	0.0286	Knurled	Cracking
33	7252	0.875	60	1.0	600	0.500	0.833	0.0500	0.0286	Knurled	No Cracking
34	7252	0.875	50	1.0	600	0.500	0.748	0.0501	0.0296	Knurled	No Cracking
35	7252	0.875	50	1.0	700	0.500	0.751	0.0500	0.0297	Knurled	No Cracking
36	7252	0.875	60	1.0	700	0.500	0.835	0.0500	0.0286	Knurled	No Cracking
37	7252	0.875	70	1.0	700	0.500	0.949	0.0501	0.0286	Knurled	Incipient Cracking
38	7252	0.875	80	1.0	800	0.500	1.135	0.0500	0.0287	Knurled	Cracking
39	7252	0.875	70	1.0	800	0.500	0.955	0.0501	0.0281	Knurled	Incipient Cracking
40	7252	0.875	60	1.0	800	0.500	0.834	0.0500	0.0276	Knurled	No Cracking
41	7252	0.875	50	1.0	800	0.500	0.748	0.0499	0.0287	Knurled	No Cracking

Table 3: X-D Composites 25% TiC

Sample No.	Heat #	Sample Size	% Red.	S.R. 1/sec	Temp. deg. F	Diameter Initial	Diameter Final	Scribe Lines Initial	Scribe Lines Final	Platens	Comments
42	7264	0.500	50	1.0	600	0.500	0.726	0.0500	0.0371	Knurled	Cracking
43	7264	.500	40	1.0	600	0.500	0.666	0.0500	0.0377	Knurled	No Cracking
44	7264	0.500	45	1.0	600	0.500	0.694	0.0500	0.0372	Knurled	No Cracking
45	7264	0.500	50	1.0	700	0.501	0.732	0.0500	0.0368	Knurled	No Cracking
46	7264	0.500	60	1.0	700	0.499	0.808	0.0500	0.0365	Knurled	No Cracking
47	7264	0.500	70	1.0	700	0.500	0.913	0.0500	0.0367	Knurled	Incipient Cracking
48	7264	0.500	70	1.0	800	0.500	0.924	0.0500	0.0370	Knurled	Incipient Cracking
49	7264	0.500	80	1.0	800	0.500	1.077	0.0499	0.0335	Knurled	Cracking
50	7264	0.500	60	1.0	800	0.500	0.816	0.0499	0.0368	Knurled	Incipient Cracking
51	7264	0.500	60	1.0	600	0.500	0.803	0.0500	0.0371	Knurled	Incipient Cracking
52	7264	0.500	50	1.0	600	0.500	0.734	0.0499	0.0365	Smooth	No Cracking
53	7264	0.500	60	1.0	600	0.500	0.815	0.0499	0.0375	Smooth	Incipient Cracking
54	7264	0.500	70	1.0	600	0.500	0.915	0.0500	0.0368	Smooth	Cracking
55	7264	0.500	70	1.0	700	0.500	0.933	0.0499	0.0371	Smooth	Cracking
56	7264	0.500	60	1.0	700	0.500	0.821	0.0499	0.0368	Smooth	Incipient Cracking
57	7264	0.500	70	1.0	800	0.501	0.945	0.0500	0.0372	Smooth	Cracking
58	7264	0.500	60	1.0	800	0.500	0.829	0.0500	0.0366	Smooth	Incipient Cracking
59	7264	0.500	50	1.0	800	0.500	0.741	0.0500	0.0371	Smooth	No Cracking
60	7264	0.500	45	1.0	800	0.500	0.705	0.0500	0.0377	Smooth	No Cracking
61	7264	0.500	70	1.0	700	0.500	0.925	0.0499	0.0375	Smooth	Cracking

Table 4: X-D Composites 25% TiC

Sample No.	Heat #	Sample Size	% Red.	S.R. 1/sec	Temp. deg. F	Diameter		Scribe Lines		Platens	Comments
						Initial	Final	Initial	Final		
62	7264	0.875	50	1.0	600	0.500				Knurled	Error in Testing
63	7264	0.875	50	1.0	600	0.500	0.750	0.0500	0.0281	Knurled	No Cracking
64	7264	0.875	60	1.0	600	0.500	0.833	0.0499	0.0306	Knurled	Incipient Cracking
65	7264	0.875	70	1.0	600	0.500	0.942	0.0501	0.0285	Knurled	Incipient Cracking
66	7264	0.875	80	1.0	600	0.500	0.834	0.0499	0.0287	Knurled	Cracking
67	7264	0.875	60	1.0	700	0.500	0.834	0.0500	0.0273	Knurled	No Cracking
68	7264	0.875	70	1.0	700	0.501	0.984	0.0500	0.0285	Knurled	Incipient Cracking
69	7264	0.875	80	1.0	700	0.500	1.122	0.0500	0.0286	Knurled	Cracking
70	7264	0.875	70	1.0	800	0.500	0.957	0.0500	0.0281	Knurled	Incipient Cracking
71	7264	0.875	80	1.0	800	0.500	1.139	0.0500	0.0285	Knurled	Cracking
72	7264	0.875	60	1.0	600	0.500	0.840	0.0500	0.0296	Smooth	Incipient Cracking
73	7264	0.875	50	1.0	600	0.500	0.758	0.0500	0.0304	Smooth	No Cracking
74	7264	0.875	70	1.0	600	0.500	0.955	0.0500	0.0289	Smooth	Incipient Cracking
75	7264	0.875	80	1.0	600	0.500	1.127	0.0500	0.0293	Smooth	Cracking
76	7264	0.875	80	1.0	700	0.500	1.138	0.0500	0.0287	Smooth	Cracking
77	7264	0.875	70	1.0	700	0.500	0.955	0.0499	0.0290	Smooth	Cracking
78	7264	0.875	80	1.0	800	0.500	1.154	0.0500	0.0285	Smooth	Cracking
79	7264	0.875	90	1.0	800	0.500	1.410	0.0500	0.0309	Smooth	Cracking
80	7264	0.875	50	1.0	800	0.500	0.754	0.0500	0.0282	Smooth	No Cracking
81	7264	0.875	75	1.0	600	0.500	1.026	0.0500	0.0289	Smooth	Incipient Cracking
82	7264	0.875	65	1.0	700	0.500	0.887	0.0500	0.0291	Smooth	Cracking

Table 5: Summary of 15% and 25% TiC Workability Tests

% TiC	Temperature (deg. F)	Y-intercept
15	600	.24
15	700	.25
15	800	.30
25	600	.22
25	700	.29
25	800	.29